Fermilab

$\bar{p}$ Note #448

Comparisons of Yield Calculations With Data

G. Dugan

2/1/86

Comparisons of yield calculations with data

G. Dugan
Feb. 1, 1986

Given what is claimed to a reasonably accurate technique for calculating the pbar yield, it is useful to ask for comparisons with the data available from the recent commissioning run. The simplest comparison to make is that of the yield. The number of pbars circulating in the Debuncher was measured many times; the total number of secondaries at IC728 in AP-2 was also measured many times. The ratio of pbars to total flux at IC728 was measured once (Bk. I, p 166); this number was $\bar{p}$ /total = 0.032. Typically, the ratio of secondaries at IC728 to protons on target was about 0.0012 (this was about the same number, independent of whether the lens was operated at 600 or 1000 T/m.) Thus, at IC728 we have

$$N_p/N_{\bar{p}} \sim 1.2\times10^{-3} \times 3.2\times10^{-2} = 3.8\times10^{-5} = 38 \text{ ppm}$$

The expected momentum aperture of AP-2 is .048X8.9=.427 GeV/c, so the yield is 38/.427 = 85 ppm/GeV/c. The errors in this number can come from (a) errors in the $\bar{p}$ /total ratio, (b) errors in the IC728 flux (probably small) and (c) errors in the momentum acceptance of AP-2. The momentum dispersion of the left bend was measured to be close to the design value but the aperture limits in this region are unclear. We take the total error in the yield to be ± 20% (very optimistic).

In the Debuncher, we measured 5.3x10**6 pbars circulating in $\Delta p/p$ = 4.5%, for 10**12 protons, so the yield is $Y = 5.3\times10^6/10^{12}/.045\times8.9$ = 12 ppm/GeV/c. Errors are probably ± 40% here, again optimistically.

During the run, we typically operated with a smaller proton beam spot size than the design (because the per pulse intensity was lower than the design). Typically, σ_h was .34 mm. The effect of abberations (see ref. 1, Addendum C) adds about .26 mm in quadrature, giving σ_h about .42 mm. We ran with a target length of 7.2 cm. Fig. 1a shows the yield vs emittance for various gradients, and the points corresponding to AP-2 and the Debuncher. Note that, as observed, there should be very little difference between the yields at 600 T/m and 1000 T/m lens gradients for small emittances. The straightforward interpretation of these data are: the effective acceptance of the pbar collection and transport system up to IC728 in AP-2 is 13 ± 2 pi mm-mrad (it is supposed to be 55 pi horizontally and 30 pi

vertically). The effective acceptance of the system including the Debuncher is 5 $\pm$ 1 pi mm-mrad (it is supposed to be 20 pi).

Of course, the actual flux measured at IC728 is mostly pions. Hence it would be interesting to estimate the pion yield from the target and compare with the IC728 flux. The procedure used to do this is outlined in Appendix I. It is interesting that the results of this estimate give a ratio $\pi^- / \bar{p}$ of about 18, whereas we measured 23 (Bk. I, p. 166), which is within 30%. The measured pion yield at IC728 is estimated as follows: from Bk. I, p. 166, π^- / e^- is about 2.93, and $\pi^- / \bar{p}$ is 23, so π^-/total = .722. Using total/protons = 0.0012, π/p = 867 ppm. For $\Delta p/p$ = 4.5%, the pion yield is 2030 ppm/GeV/c at IC728. Using the decay factor of .443 (see Appendix I), this is 4582 ppm/GeV/c at the target. Figure 1b shows the predictions and data for pions; the effective emittance at IC728 is 16 $\pm$ 1 pi mm-mrad, essentially in agreement with the pbar data.

Both with the lens at 600 T/m and at 1000 T/m, measurements were made of the variation in yield with lens gradient, for a fixed target distance. These data, together with the appropriate calculations, are shown in fig. 2. The agreement is reasonable; the small shift observed may be due simply to a 5% error in calibration of the lens gradient vs. lens voltage. The fact that the data are above the curve for low gradients in the 1000 T/m target position case may be due to background (i.e., secondaries not produced in the target). The data also contains substantial electron contamination (25%).

With the lens at 600 T/m, we measured the variation in the yield vs. proton beam spot size. These data are shown (together with the prediction) in fig. 3. The error bars are supposed to reflect relative errors only and are derived from pulse-to-pulse variations. The agreement is again reasonable. The effective spot sizes for the data include the effects of the abberations mentioned above.

With the lens at 1000 T/m, we measured the variation in the yield vs. target length. This is shown, together with the calculation, in fig. 4. The normalization of the data is arbitrary. The agreement in shape is seen to be reasonable. Also with the lens at 1000 T/m, we measured the variation of the yield vs. lens vertical position. The relationship between a shift of the lens axis and a shift of the proton beam spot on target is derived in Appendix 2: the result is $\delta x_{lens} = 1.14\, \delta x_{targ}$. In fig. 5, we show the data for the yield variation with lens motion, and the prediction for the yield variation with target motion. The

normalization of the data curve is again arbitrary. The data curve is somewhat broader than the predictions; again, this may be related to the electron contamination, which is presumably a more diffuse source than the hadrons.

With the lens at 600 T/m, the dependence of the yield on lens timing was explored. This dependence is due to a change in the lens gradient and a change in the lens aberrations. As explained in ref. 1, Addendum C, the deviation of the lens field from linearity can be crudely modeled as an effective increase in the proton beam spot size on the target. Fig. 6 shows the rms aberration vs phase (from ref. 1, Addendum C), the measured variation of the yield vs phase, and a crude prediction, based on the calculated yield variation with σ_n (proton beam spot size), adding the aberration effect ($\Delta_{rms} R_0$) in quadrature. The effect of the variation in gradient (also shown in fig. 6) has not been included. As the fig. shows, there is surprisingly good agreement with the prediction, both in the optimum phase and in the variation of the yield with phase. The asymmetry in the comparison of the yield variation about the optimum is presumably related to the fact that the gradient falls off quickly for large phases but rises slightly for small phases.

All the comparisons in figs. 2 to 6 would obviously be better if made using pbars circulating in the Debuncher. This data should be taken during the next run. Additionally, the planned Cerenkov counter at IC728, which can separate out the electrons, pions and pbars, can be used to sharpen the comparisons.

The major piece of information from this analysis comes from the data shown in figs. 1a and 1b. If the "straightforward" interpretation mentioned above is correct, then there is a major aperture restriction in AP-2 before IC728. The acceptance should be well in excess of 20 pi, but looks like about 15 pi. Alternatively, our assumption about the momentum acceptance of AP-2 could be in error; if it is much smaller than we expect, then the yield could be correct and the AP-2 acceptance large. However, this is unlikely: we measure 4.5% momentum spread in the Debuncher. Moreover, for a large acceptance, we would have expected a more dramatic dependence of the yield on lens gradient (see figs 1a and 1b), which was not observed.

The other implication of this data is the following. If we believe that the Debuncher acceptance is really about 10 pi, then we would expect a yield of about 55 ppm/GeV/c (from fig. 1a), not 12 ppm/GeV/c. The loss of a factor of 55/12 $\sim$ 4.6 must be either in AP-2 downstream of IC728, in the

Debuncher injection channel, or in the first few turns of the Debuncher, due to a mismatch at injection. This mismatch would have to correspond to an emittance dilution of about a factor of 2 in each plane

These considerations can be summarized in a revised "missing factor" table for the system from the target to circulating beam in the Debuncher:

STAGE	DESIGN YIELD (ppm/GeV/c) into 20π mm-mrad	MEASURED YIELD (ppm/GeV/c)	MISSING FACTOR CUMULATIVE	MISSING FACTOR INDIVIDUAL
TARGET, LENS, AP-2 to IC728	130	85	1.5	1.5 (1)
DEBUNCHER CIRCULATING BEAM	130	12	10.8	7.2 (2)

(1) This factor is what we are missing to get 20 pi to IC728. In fact, since AP-2 should be able to transmit 55 pi horizontally and 30 pi vertically, we should expect a considerably larger number (like 260 ppm/GeV/c) at IC728; hence the missing factor relative to the design is more like 3.

(2) This factor of 7.2 presumably is comprised of a factor of about 1.6 from the difference in acceptance between the 15 pi at IC728 and the 10 pi in the Debuncher; and a factor of 4.6 due to beam loss after IC728 and emittance dilution in the Debuncher.

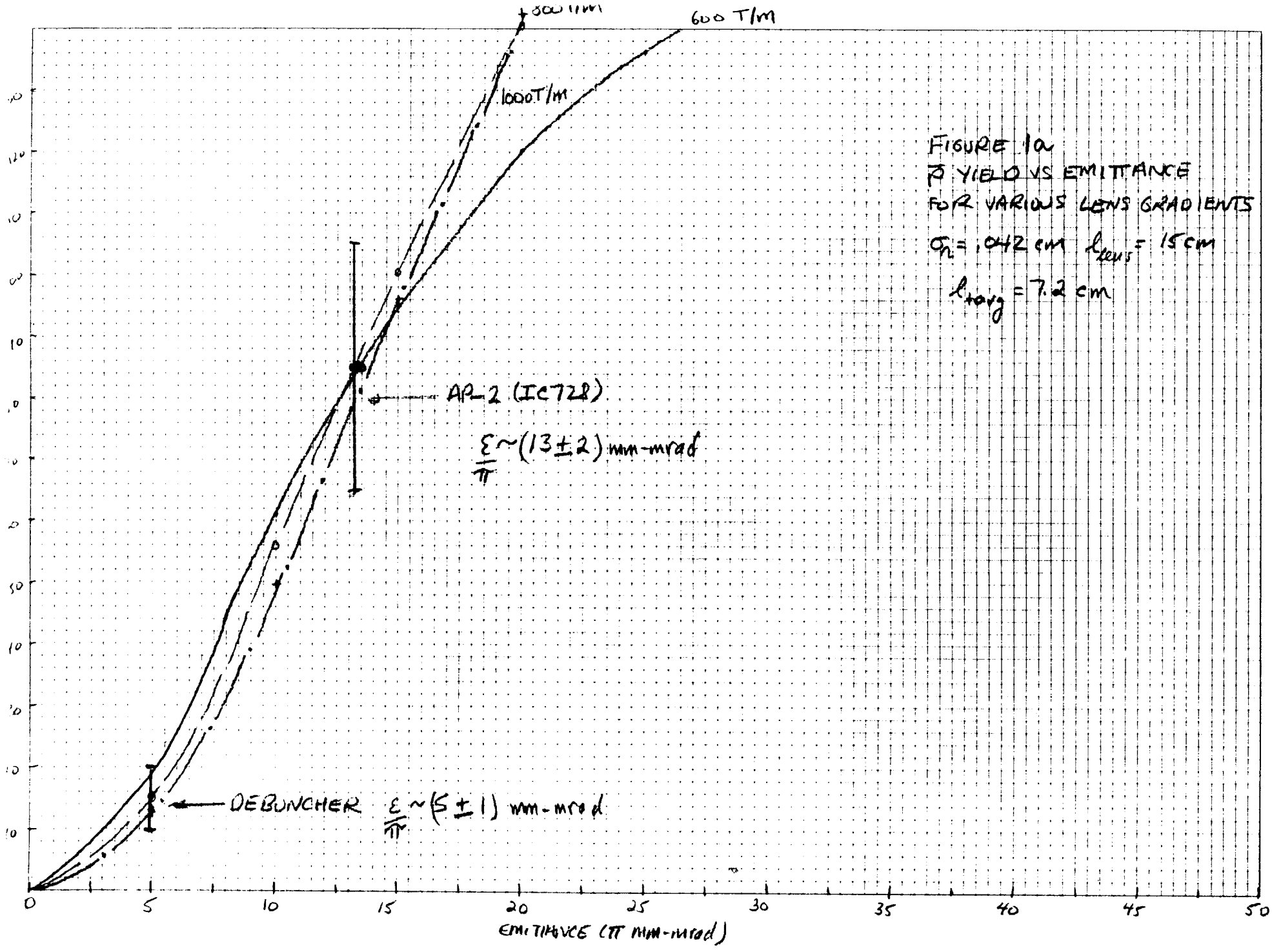

FIGURE 1a
$\bar{p}$ YIELD VS EMITTANCE
FOR VARIOUS LENS GRADIENTS
$\sigma_z = .042$ cm $\ell_{lens} = 15$ cm
$\ell_{targ} = 7.2$ cm

K+E 10 X 10 TO THE INCH • KEUFFEL & ESSER CO.
46 0660

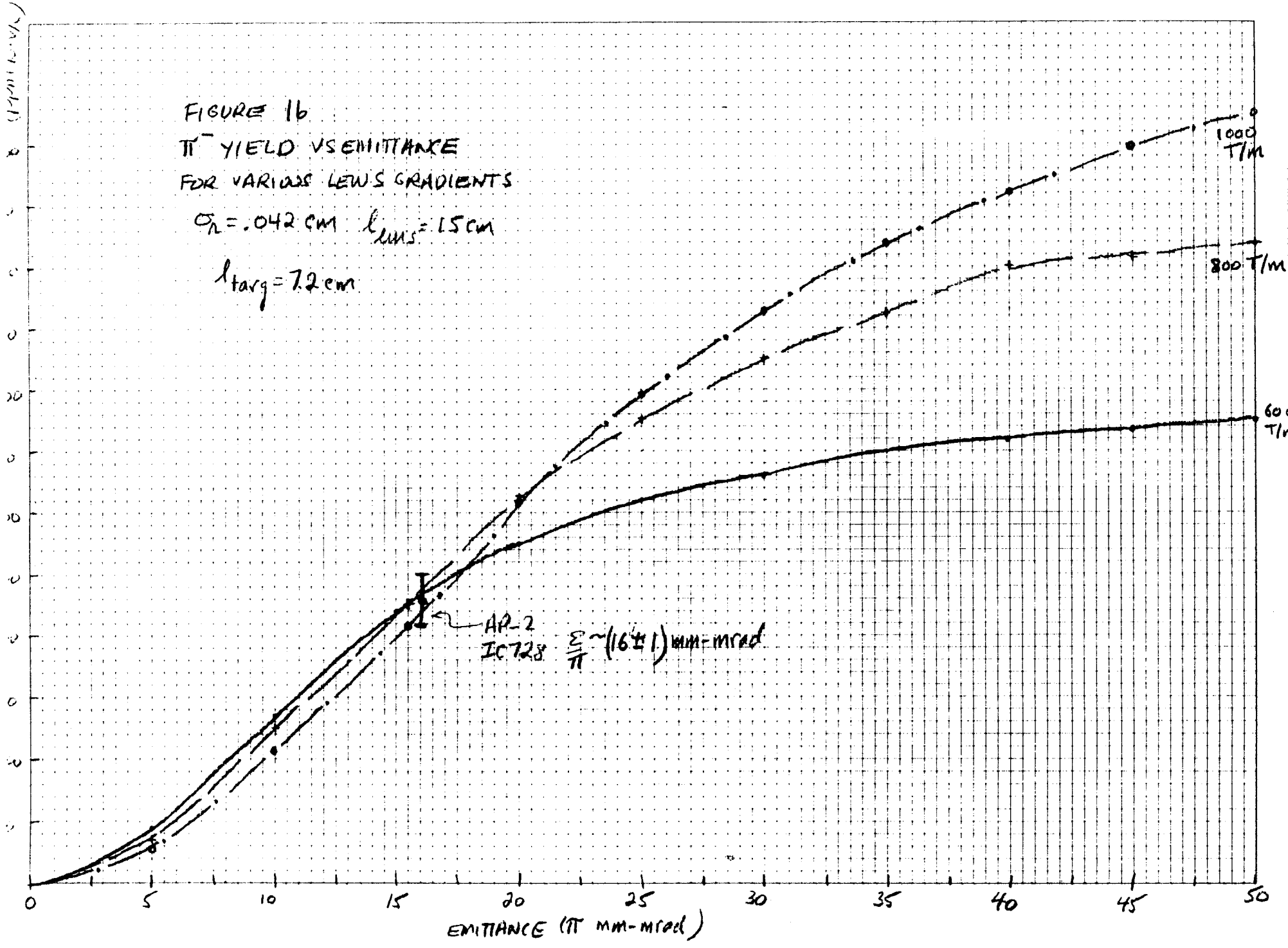

46 0660
K+E 10 X 10 TO THE INCH
KEUFFEL & ESSER CO.

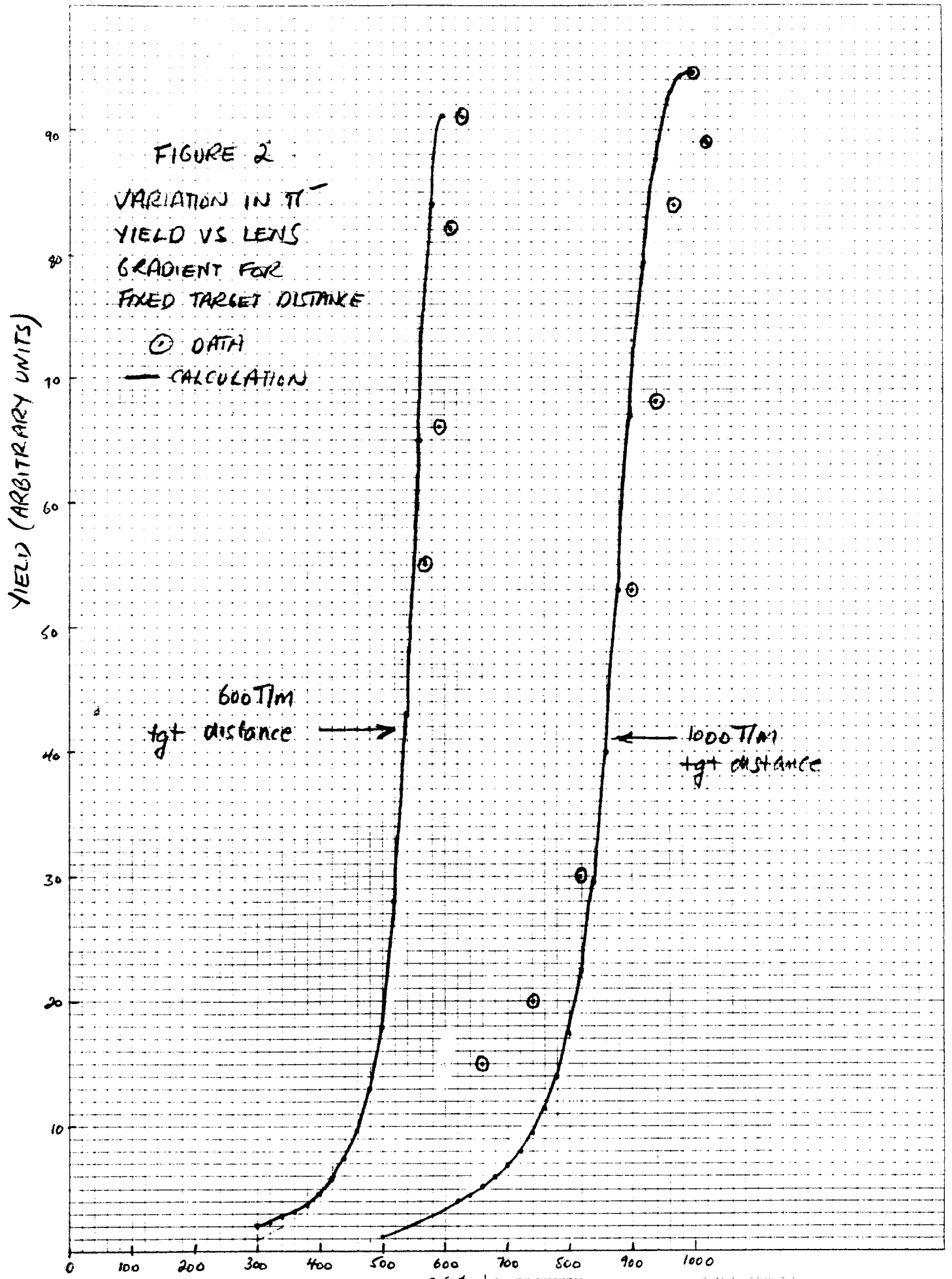

46 0660
K+E 10 X 10 TO THE INCH
KEUFFEL & ESSER CO.

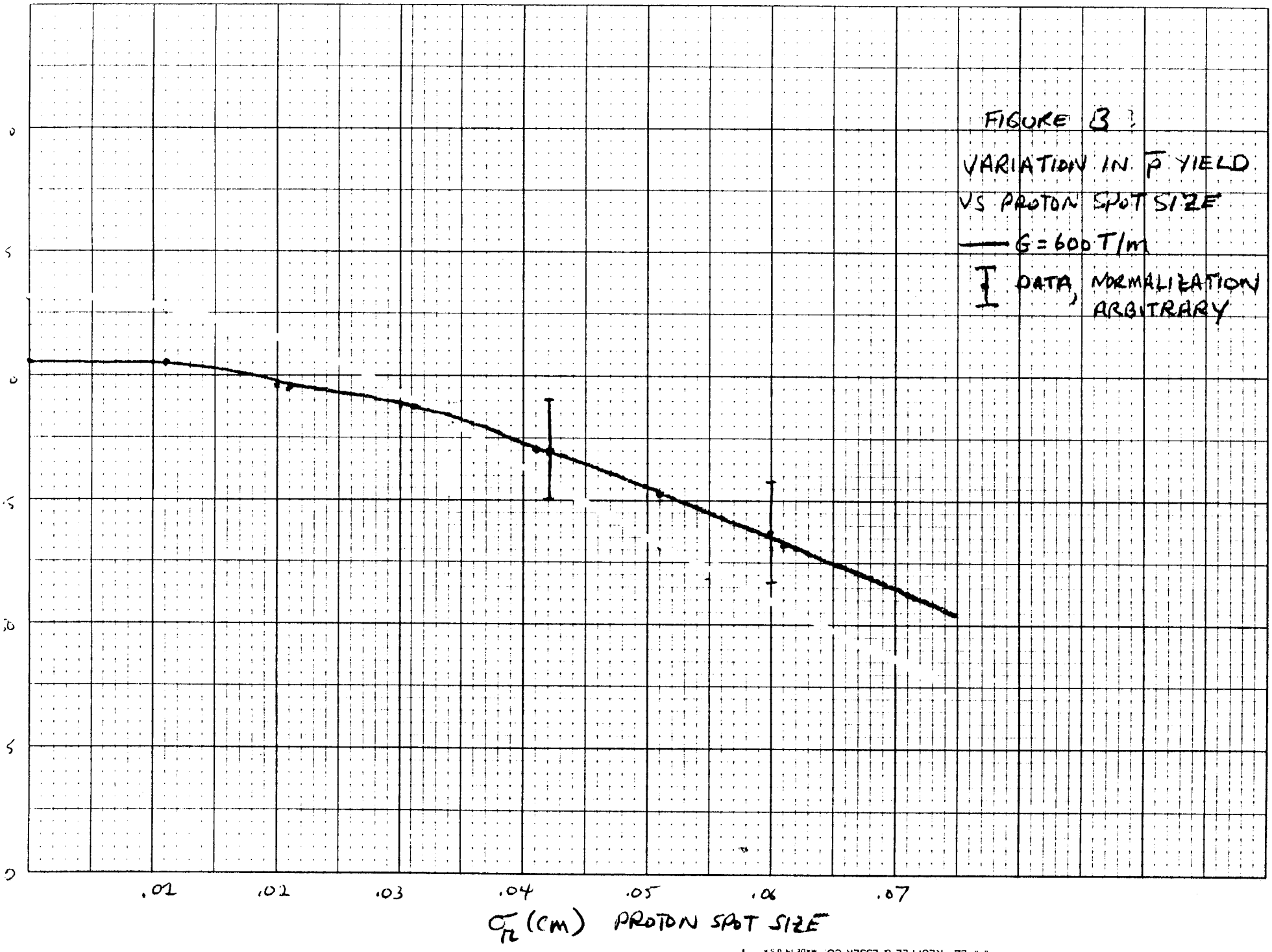

K+E 10 X 10 TO THE INCH • 7 X 10 INCHES
KEUFFEL & ESSER CO. MADE IN U.S.A.
46 0780

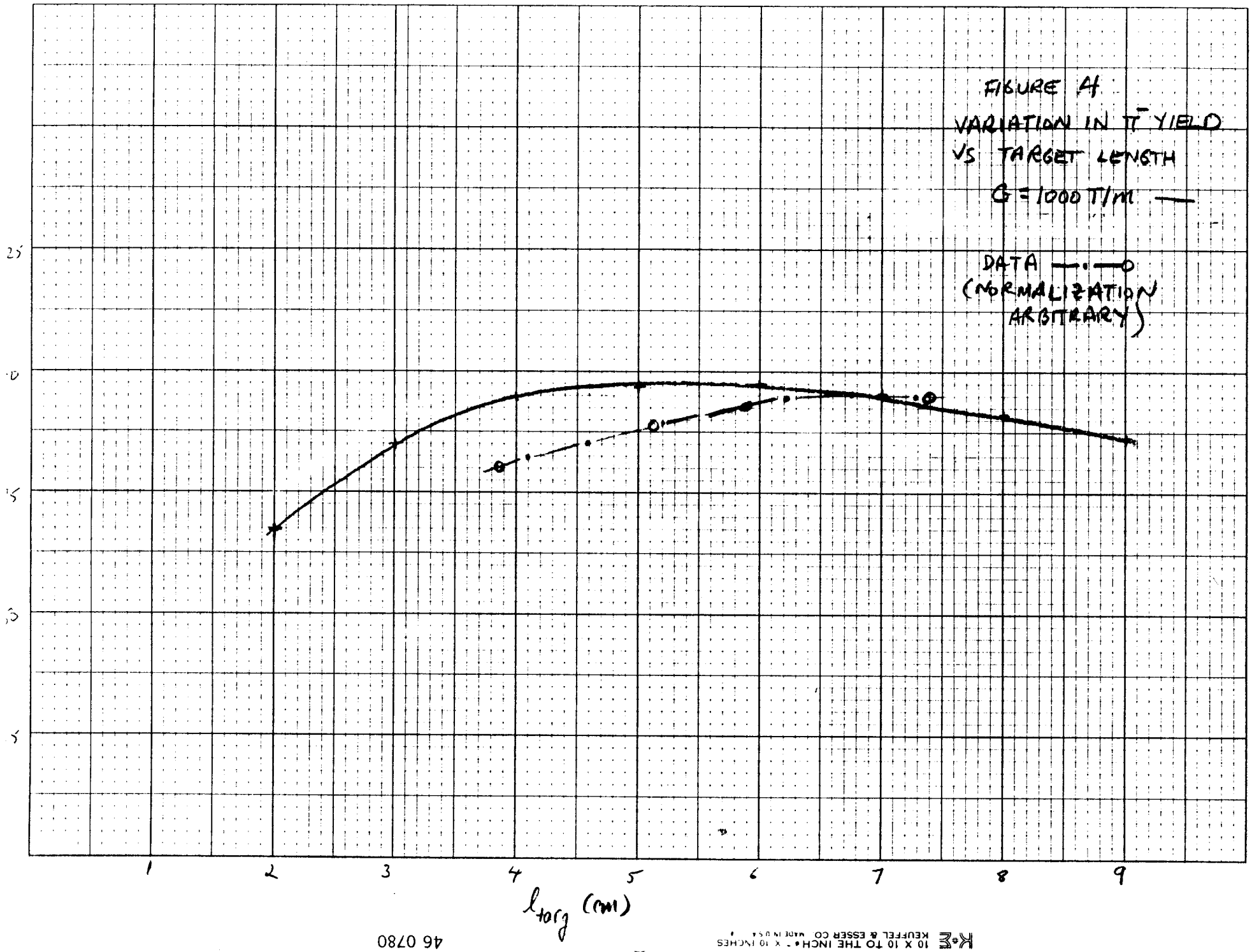

K+E 10 X 10 TO THE INCH • 7 X 10 INCHES
KEUFFEL & ESSER CO. MADE IN U.S.A.
46 0780

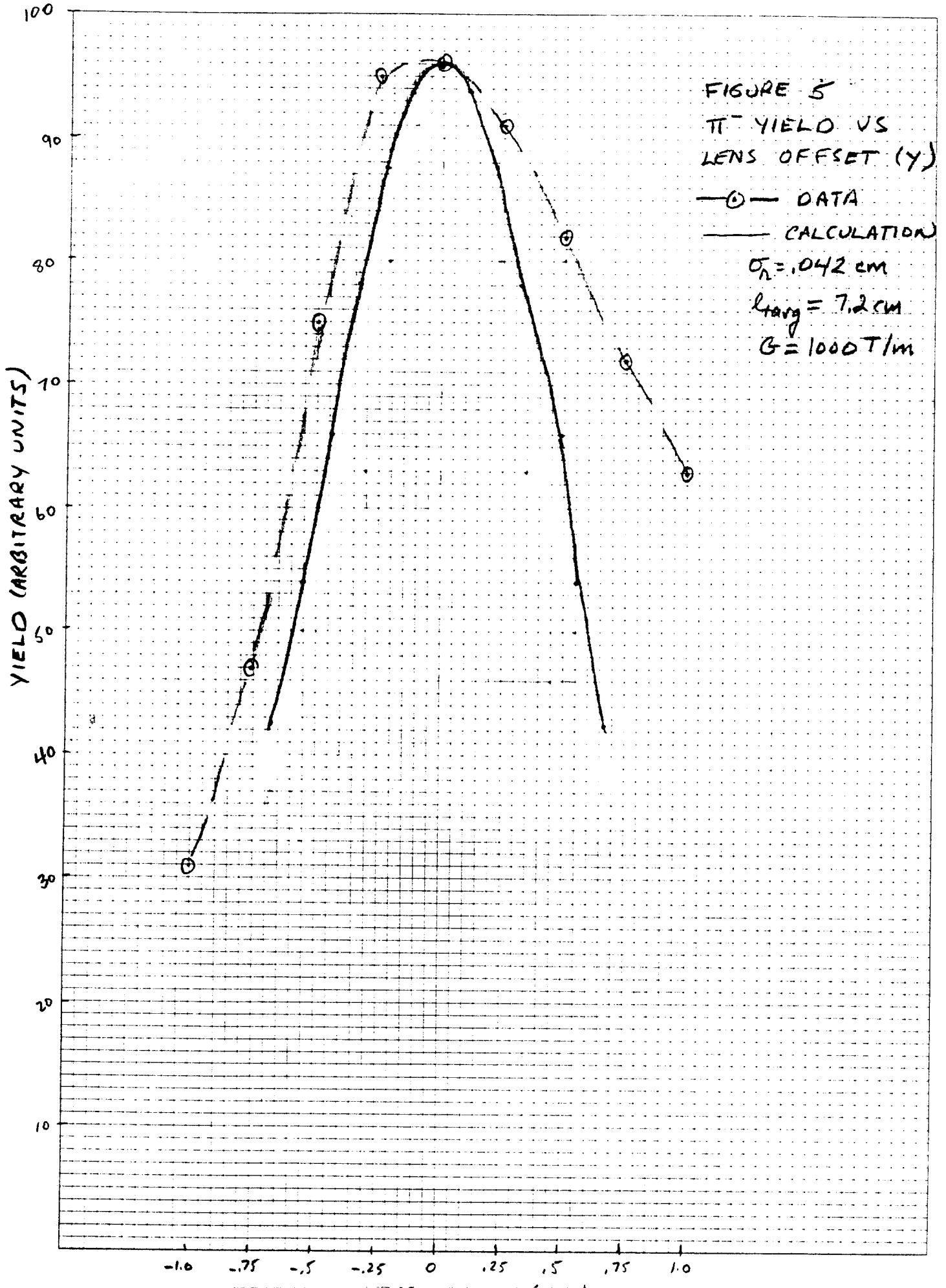

46 0660
K+E 10 X 10 TO THE INCH
KEUFFEL & ESSER CO.

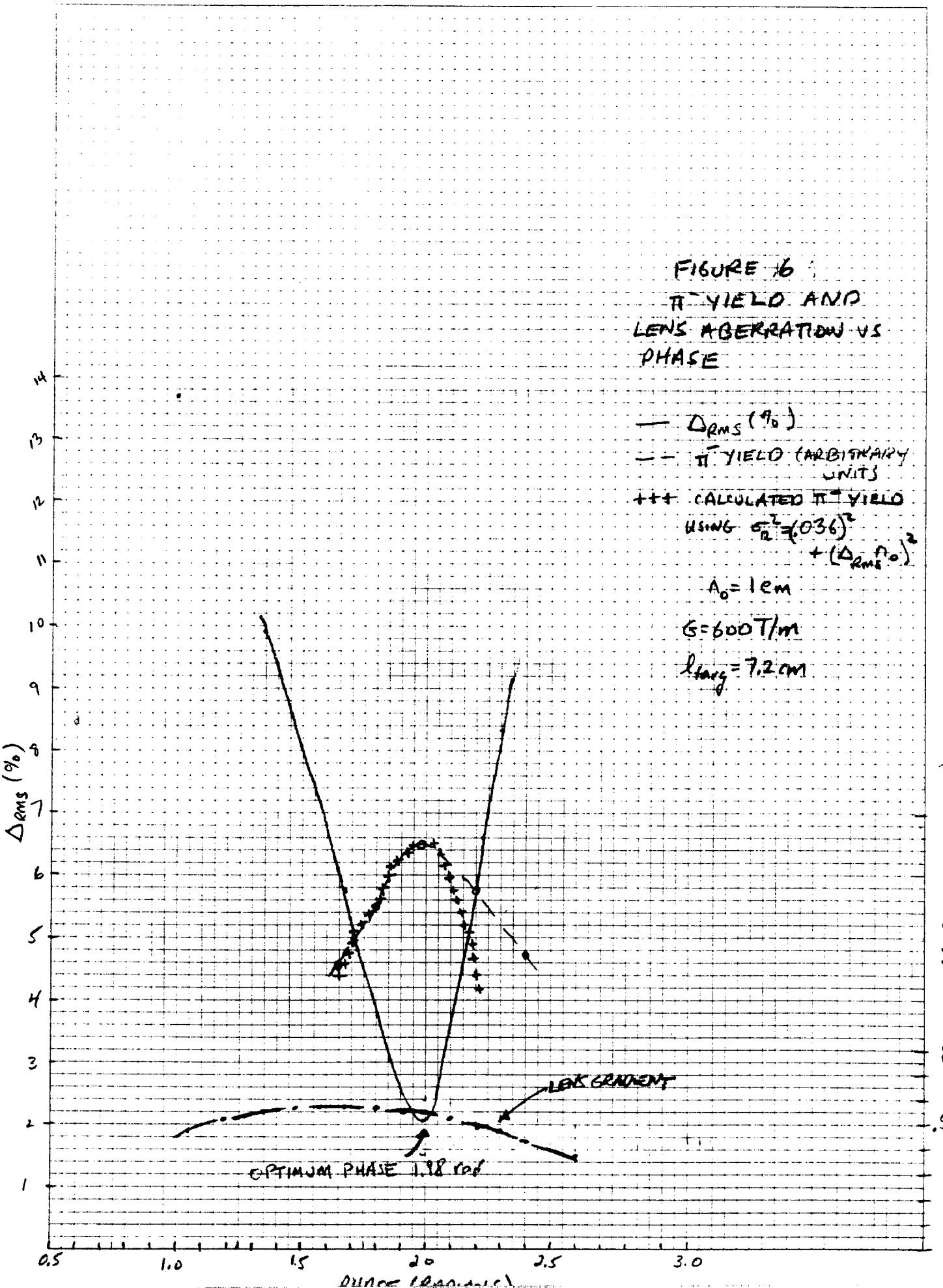

46 0660

K+E 10 X 10 TO THE INCH KEUFFEL & ESSER CO.

APPENDIX I

<u>Production and collection of other secondaries</u> ($\pi^\pm, K^\pm, p, \pi^0(e^\pm)$)

To make estimates of the production rates for other secondaries, we rely on the results of D.C. Carey et al (PRD, 14, 1317 (1976)). The production cross section on hydrogen is fitted to a p_t dependence of

$$E\frac{d^3\sigma}{dp^3} = \frac{A}{(1+p_t^2/m^2)^q} \quad \text{at fixed } x_R.$$

From the table data given in the paper (see fig A-1), the following table of p_t-dependence factors (A, m^2, q) at the appropriate $x_R(0)$ for the particle (computed from the kinematic equations in Appendix A-1) of $R=1$ can be assembled

Particle	$x_R(0)$	A (mb/GeV^2)	m^2 (GeV^2/c^2)	q	m/p (mrad)	$\bar{\theta}$ (mrad) (Hydrogen)	σ_{tot} (mb) (H
π^+	.074	43.5	.34	3.54	65.5	32.4	[redacted]
K^+	.088	3.4	.42	3.21	72.8	39.4	[redacted] 17.
π^-	.074	27.0	.42	3.60	[redacted] 72.8	35.5	[redacted] 2
K^-	.088	1.6	.62	3.47	[redacted] 88.5	44.6	[redacted] 22
π^0	.074	13.0	.52	3.50	[redacted] 81.0	40.5	—
p	.125	3.4	1.08	4.70	116.8	46.2	[redacted] 40
$\bar{p}$	.125	.635	1.24	4.58	125.1	50.4	[redacted] 57

$\bar{\theta}$ is computed from $\bar{\theta} = \frac{m}{p}\sqrt{\frac{1}{2q-3}}$, appropriate for the form of $\frac{d^3\sigma}{dp^3}$ mentioned above. The last column gives the total cross section on hydrogen, at $P_{Lab} = 8$ GeV/c. For $\bar{p}p$ production on hydrogen, the numbers can be compared with eH's equation

$$E/\sigma_{obs}\frac{d^3\sigma}{dp^3} = k(1-x_R)^8 \exp(-3p_t^2), \quad k = .065$$

For fixed x_R $\quad \theta_0 = \bar{\theta} = \sqrt{\frac{1}{3p^2}} = 65$ mrad (30% larger than above)

The normalization is $N = k\,\sigma_{abs}\,(1-x_R)^8$ $\quad \sigma_{abs} \sim 32$ mb $\quad x_R = .125$

$N = .714$ to be compared with .635 in the table above (12% high)

In order to estimate the yields for other particles, we need the production cross sections on tungsten, and the absorption lengths in tungsten. We proceed as follows

(1) We take the same "target-dependent" P_t, x_R dependences as specified by CH in reference . For the P_t dependence of the hydrogen cross sections, of the form $\exp(-\gamma_x P_t^2)$, we argue that, for particle x,

$$\gamma_x = \frac{1}{P^2 \bar{\theta}_x^2}. \quad \text{For } \gamma_{\bar{p}}, \text{ we take from CH } \gamma_{\bar{p}} = 3.$$

For other x, we scale $\gamma_x \bar{\theta}_x^2 = \gamma_{\bar{p}} \bar{\theta}_{\bar{p}}^2$

$$\gamma_x = \gamma_{\bar{p}} \left(\bar{\theta}_{\bar{p}} / \bar{\theta}_x\right)^2,$$ using the numbers for $\bar{\theta}$ from the above table,

(2) To get the normalization in $\frac{d^2N_x}{d\Omega\, dp} = \left(\frac{d^2N_x}{d\Omega\, dp}\right)_{0^\circ} e^{-\theta^2/\bar{\theta}^2}$,

we scale $\left(\frac{d^2N_x}{d\Omega\, dp}\right)_{0^\circ} = \left(\frac{d^2N_{\bar{p}}}{d\Omega\, dp}\right)_{0^\circ} \times \left(\frac{A_x}{A_{\bar{p}}}\right)$ from the above table.

(3) To get the angular dependence we include the P_t dependence from part (1) above, the x_R dependence of the hydrogen cross sections (from the PR article: $(1-x_R)^n$) and the x_R and P_t target-dependences. We compute $\sqrt{\bar{\theta}^2}$ ~~for the total~~ including all these dependences. The results are

Particles	$x_R(0^\circ)$	$\left(d^2N_x/d\Omega\, dp\right)_{0^\circ}$	n	(mR) $\sqrt{\bar{\theta}^2}$ (total)	$\bar{\lambda}$ (cm)
π^+	.074	17.263	4.2	45	15.78
K^+	.088	1.348	4.9	56.5	22.54
π^-	.074	10.71	6.0	49.5	14.60
K^-	.088	.635	5.1	66.1	17.53
π^0	.074	5.17	7.0	57.5	—
p	.125	1.35	8	66.5	9.86
$\bar{p}$	.125	.252	8	74.2	9.29

The values for $\bar{\lambda}$(cm) in the above table were computed by scaling using the hydrogen total cross sections, using

$$\bar{\lambda}_x = \lambda_p (\sigma_p/\sigma_x) \quad , \text{ with } \lambda_p = 9.86 \text{ cm. For } \bar{p}, \text{ the}$$

number 9.29 cm, from ett paper, was used.

Using the above values of $\bar{\theta}$, $d^2N/d\Omega dp|_{0°}$, and $\bar{\lambda}$ for each particle, yield calculations are possible for each type. The "relative yields" and decay factors (to IC728) are given in the following table

Particle	$d^2N/d\Omega dp\|_{0°}$ (relative)	Yield (relative)	Decay	Product
π^+	68.50	.924	.443	28.0
K^+	5.35	1.06	.132	.748
π^-	42.5	.970	.443	18.3
K^-	2.52	1.11	.132	.369
π^0	20.52	—	—	—
p	5.36	.9858	1	5.28
$\bar{p}$	1	1	1	1

The first column is the ratios of the forward cross sections from the previous table. The second column is the relative yields (for the same $d^2N/dp d\Omega|_{0°}$), which takes into account the differences in $\bar{\theta}$ and $\bar{\lambda}$ shown in the previous table. The yields are into 20π emittance, with the nominal target and lens parameters. The third column is the decay factor $f = 1 - \exp(l/l_0)$, $l_0 = \beta\gamma c \tau_0$ with $\tau_0 = 25$ nsec for $\pi^\pm$, 12.4 nsec for $K^\pm$; $\beta\gamma = p/m = 18.0\ (K^\pm)$, $63.6\ (\pi^\pm)$ l is the distance to IC728 (290 m).

From the "product" column, we predict (at IC728) the following:

$\pi^-/\bar{p} = \underline{18.0}$ (we measured 23.2)

$K^-/\bar{p} = \underline{.37}$

Measured: $\pi^-/e^- = 2.93$ $(\pi^-/e^- > \pi^-/\pi^0 = 18.3/20.52 = .89)$

Total negatives $\pi^- + K^- + \bar{p} + e^- = 18 + .37 + 1 + 18/2.93 = \underline{25.5}$ $\bar{p}/tot = \underline{.039}$

$p/\bar{p} = \underline{5.3}$

~~Total pos~~ $\pi^+/p = 28/5.3 = \underline{5.3}$

$K^+/p = .748/5.3 = \underline{.141}$

Total positives $K^+ + \pi^+ + p + e^+ = 28 + .75 + 5.3 + 18/2.93$

(assume $e^+ = e^-$) $= \underline{40.2}$ $p/tot = \underline{.132}$

total $+/- = 40.2/25.5 = \underline{1.58}$

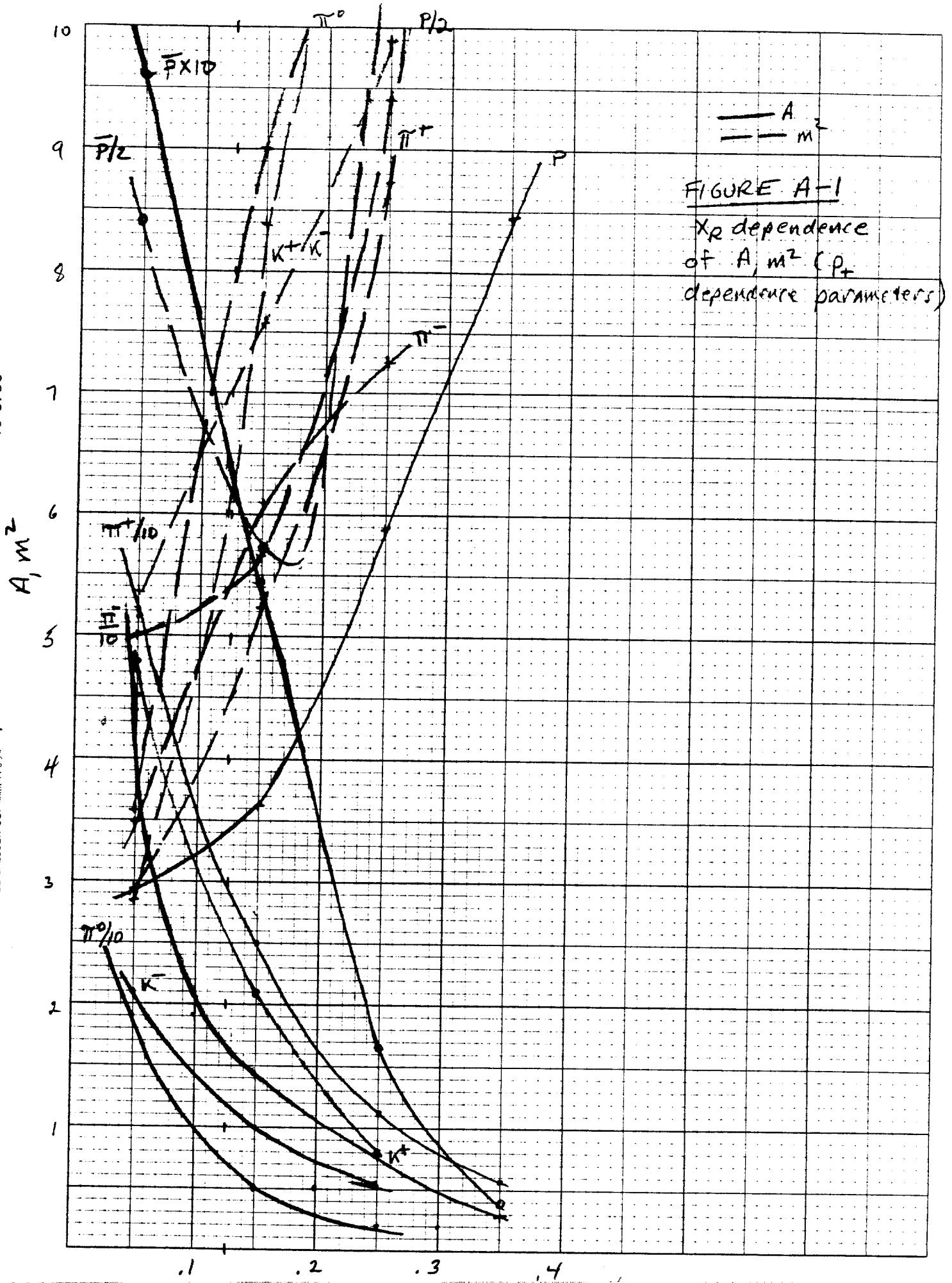

46 0780
K+E 10 X 10 TO THE INCH • 7 X 10 INCHES KEUFFEL & ESSER CO. MADE IN U.S.A.

APPENDIX II

Lens shift

$\vec{B}(r) = B_0 (r/r_0)\,\hat{\theta}$ $\qquad \hat{\theta}$:

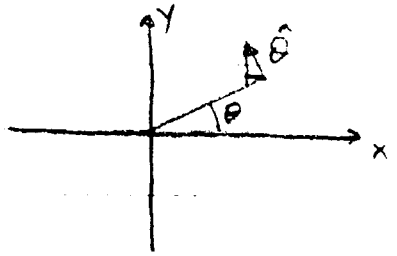

$$\hat{\theta} = \hat{y}\cos\theta - \hat{x}\sin\theta$$

$\vec{B}_x(r) = -B_0 r/r_0 \sin\theta \qquad r\sin\theta = x$

$\quad = -B_0 x/r_0\,\hat{x}$

$\vec{B}_y(r) = B_0 y/r_0\,\hat{y}$

Shift axes:

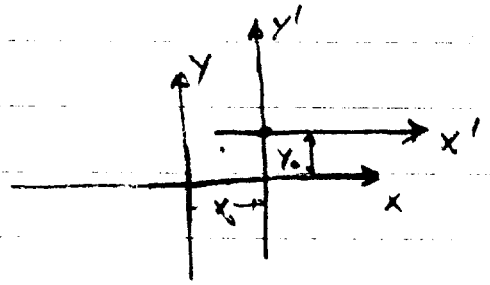

$x \to x' = x + x_0$

$y \to y' = y + y_0$

$$B_x = -B_0/r_0\,(x + x_0) = -\frac{B_0 x}{r_0} - \frac{B_0 x_0}{r_0}$$

Lens action $mv\,d^2x/ds^2 = -eB(x)$

$$d^2x/ds^2 = -e/p\left(\frac{B_0 x}{r_0} + B_0 x_0/r_0\right)$$

$$\frac{d^2x}{ds^2} + k^2 x = -k^2 x_0 \qquad k^2 = eB_0/p$$

$x(s) = x_c(s) + \delta s^2 \qquad \ddot{x}_c = -k^2 x$

So $\ddot{x} = \ddot{x}_c + 2\delta = -k^2 x + 2\delta, \qquad 2\delta = -k^2 x_0$

Let x_0, x_0' = coords at entrance to the lens

x_1, x_1' = " " exit from lens $\qquad s = \ell$

$$x_1 = \cos\mu x_0 + 1/k \sin\mu\, x_0' + \delta\ell^2$$

$$\dot{x}_1 = -k\sin\mu x_0 + \cos\mu x_0' + 2\delta\ell$$

$$\delta = -\frac{k^2 x_0}{2}$$

So $\delta\ell^2 = -\dfrac{k^2 x_0 \ell^2}{2} = -\dfrac{(k\ell)^2 x_0}{2} = -\dfrac{\mu^2 x_0}{2} \qquad \delta\ell = \dfrac{-k^2 x_0 \ell}{2}$

For point at target x_t, x_t': $x_0 = x_t + x_t' f$

$$x_0' = x_t'$$

So $x_i = \cos\mu (x_t + x_t' f) + x_t' \sin\mu / k + \delta l^2$

$$x_i' = -k \sin\mu (x_t + x_t' f) + \cos\mu \, x_t' + 2\delta l$$

at image point: $x_i = x_t'/k\sin\mu + \delta l^2 + 2\delta l f$

$$x_i' = -x_t k \sin\mu + 2\delta l$$

So $x_t = \dfrac{x_i' - 2\delta l}{-k\sin\mu} = \dfrac{x_i'}{-k\sin\mu} + \dfrac{2\delta l}{k\sin\mu}$

$$x_t' = x_i k \sin\mu - (\delta l^2 + 2\delta l f) k \sin\mu$$

Center of lens acceptance ($x_i' = x_i = 0$) transforms back at image

at target to $x_{t_0} = +\dfrac{2\delta l}{k\sin\mu} = +\dfrac{2l}{k\sin\mu}\dfrac{k^2 x_0}{2} = +\dfrac{k l x_0}{\sin\mu} = \dfrac{\mu x_0}{\sin\mu}$

for $k = .058\ \text{cm}^{-1}$ $l = 15$ cm $\mu = .87$

$$\underline{x_{t_0}} = \frac{.87}{.76} x_0 = \underline{1.14\, x_0}$$

$$x_{t_0}' = -\delta l^2 + 2\delta l f \cdot k\sin\mu$$

$$= +\delta l(l+2f)\frac{k^2 x_0}{2} k\sin\mu$$

$$= \frac{k^3 l(l+2f)}{2} \sin\mu \, x_0$$

$$= \frac{(.058)^3 (15)(15+2\times 14)}{2} \sin .87 \, x_0$$

$$= .049\, x_0 (\text{cm})$$